

# A Novel One-Dimensional Chaotic System and Its Application in Chaotic Communication Systems

Linhan Feng\*

School of Electronic and Information Engineering, Beijing Jiaotong University, Beijing, China, 100044

\*Corresponding author: 23721008@bjtu.edu.cn

**Abstract.** Chaotic systems are widely applied in secure communications, and one-dimensional (1D) chaotic systems are preferred for resource-constrained scenarios due to their structural simplicity and ease of hardware implementation. However, traditional 1D systems (Logistic, Sine, Chebyshev maps) suffer from narrow/discontinuous chaotic intervals, insufficient sequence complexity, and weak initial sensitivity, leading to chaotic degradation in digital implementation and poor communication performance in practical channels. To address these issues, this paper proposes a novel 1D Sin-Coupled Nonlinear Map (1D-SCNM) based on “nonlinear fusion + parameter coupling”. It retains the low-complexity advantage of 1D systems while achieving wide continuous chaotic intervals, high-complexity sequences, and strong initial sensitivity. Evaluated via bifurcation diagrams, Lyapunov exponents (LE) and sample entropy (SE), 1D-SCNM was applied as a carrier in DCSK/NR-DCSK systems, with BER tested under AWGN and Rayleigh fading channels. Results show 1D-SCNM’s chaotic interval covers full parameters (LE/SE exceeding traditional systems); NR-DCSK ( $P=16$ ) achieves a BER of  $2.3 \times 10^{-3}$  (14 dB  $E_b/N_0$ , AWGN), 97.2% improvement over DCSK (15.46 dB gain), with stable advantages in Rayleigh channels. This work provides a high-performance, easily implementable chaotic carrier for secure communications.

**Keywords:** 1D-SCNM, Chaotic Communication, Nonlinear Fusion.

## 1. Introduction

Chaos theory, as a core branch of nonlinear science, demonstrates irreplaceable application value in fields such as secure communication, image encryption, and random number generation[1][2], owing to its three essential characteristics: sensitivity to initial conditions, topological mixing, and dense periodic orbits[3][4]. Among these, one-dimensional chaotic systems (such as the Logistic and Sine maps) have become the preferred chaotic carriers for low-power communication terminals and wireless sensor networks due to their mathematically simple models, low computational complexity, and manageable hardware implementation costs (compatible with resource-constrained platforms like FPGAs and MCUs)[5][6]. The output sequences of chaotic systems, owing to their pseudo-randomness and unpredictability, can serve as reliable carriers for secure communication. Their complex behavior effectively conceals confidential data and aligns closely with the core characteristics of pseudorandom number generators, thereby providing fundamental safeguards for communication security[7][8].

Nevertheless, existing 1D chaotic systems suffer critical limitations in engineering practice. This study analyzes three representative systems (Logistic, Sine, Chebyshev) from mathematical modeling, chaotic dynamics, and performance bottlenecks to guide the proposed 1D-SCNM design. First, chaotic intervals are narrow and discontinuous[9]: for instance, Logistic map exhibits chaotic behavior only within  $a \in [0.75, 1.0]$ , while the chaotic interval for the Sine map is restricted to  $c \in [0.87, 1.0]$ . Minimal deviations in parameters or the finite precision of digital platforms may trigger periodic/steady-state degradation[10]. Secondly, chaotic sequences exhibit insufficient complexity: Lyapunov exponents (LE) in traditional systems are generally below 0.8 (e.g., the maximum LE of the Logistic map is approximately 0.69), while sample entropy (SE) often falls below 1.2. This renders predictable sequences vulnerable to attack[11][12]. Finally, weak initial sensitivity: This results in the system failing to suppress noise through the chaotic butterfly effect, leading to high

bit error rates in channels containing white Gaussian noise/Rayleigh fading[13]. Prior improvement strategies (multi-system coupling, random perturbation, piecewise mapping) either increase control complexity or fail to resolve discontinuous chaos, unable to balance 1D structural simplicity with superior performance[14].

To address these gaps, this paper proposes a novel 1D Sin-Coupled Nonlinear Map (1D-SCNM), with its core innovation rooted in “nonlinear fusion[15] + parameter coupling. By integrating the boundedness of sine transformations and nonlinear adjustability of polynomial terms, 1D-SCNM retains 1D systems’ low-complexity merit while achieving three breakthroughs:

- 1) A broad, continuous chaotic interval with robust parameter adaptability, overcoming traditional systems’ narrow chaos bottleneck;
- 2) Significantly enhanced sequence complexity (elevated LE and SE), strengthening anti-cracking capability;
- 3) Reinforced initial sensitivity to mitigate channel noise interference.

To validate 1D-SCNM’s efficacy, theoretical analysis and experimental simulation are combined: its chaotic dynamics are evaluated via bifurcation diagrams, LE, and SE; its engineering utility is verified as a carrier in DCSK/NR-DCSK systems, with BER performance tested under AWGN and Rayleigh fading channels.

This paper is structured as follows: Chapter 2 elaborates on traditional 1D systems’ limitations; Chapter 3 details 1D-SCNM’s mathematical model and core traits; Chapter 4 evaluates its chaotic performance; Chapter 5 verifies its communication application value; Chapter 6 concludes and outlines future directions.

## 2. Analysis of Traditional One-Dimensional Chaotic Systems

### 2.1. Mathematical Models of Typical One-Dimensional Chaotic Systems

#### 2.1.1 Logistic Map

The logistic map, originally employed for modelling population growth, is the most widely applied one-dimensional chaotic system[16]. Its expression is:

$$x_{n+1} = a \cdot x_n(1 - x_n) \quad (1)$$

Here,  $x_n \in (0,1)$  denotes the state variable, while  $a \in [0,4]$  represents the control parameter. Chaotic behaviour manifests only when  $a \in [0.75,1.0]$ . Beyond this range, the system converges towards either a periodic point or a steady-state value.

#### 2.1.2 Sine Mapping

The sine mapping achieves non-linear behaviour through sine transformation, with its output range possessing inherent boundedness[17]. Its expression is defined as:

$$x_{n+1} = c \cdot \sin(\pi x_n) \quad (2)$$

Here,  $x_n \in (0,1)$  and  $c \in [0,1]$  are control parameters. The sine map, owing to its simplicity and explicit nonlinear mechanism, serves as the standard model for investigating sine-based nonlinear dynamics. It finds exploratory applications in domains requiring specific distribution characteristics, such as the construction of chaotic confidentiality and weak random sources. However, the chaotic interval is confined solely to  $c \in [0.87,1.0]$ , with the output sequence concentrated within the interval  $[0.5,0.8]$ , exhibiting poor uniformity of distribution.

#### 2.1.3 Chebyshev Map

Chebyshev mapping is constructed based on the nonlinear characteristics of trigonometric functions[18]. The expression for this map is:

$$x_{n+1} = \cos(b \cdot \arccos(x_n)) \quad (3)$$

Here,  $x_n \in [-1,1]$  and  $b \in [1,4]$  serve as control parameters. Whilst this system exhibits chaotic behaviour across a broad parameter range, it suffers from strong output sequence correlation and is prone to dynamical degradation during digital implementation.

## 2.2. Quantification of Performance Shortcomings in Traditional Systems

To precisely identify the shortcomings of the traditional system, the core performance metrics of the three systems (chaotic interval characteristics of bifurcation diagrams and chaotic criteria of Lyapunov exponents) were simulated using MATLAB. The results are presented in Figure 1.

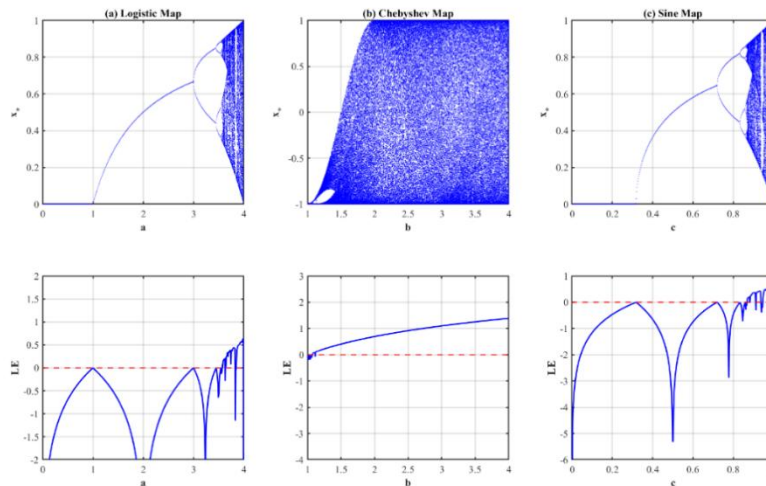


**Figure.1.** The bifurcation diagrams and Lyapunov exponents of (a) the logistic map, (b) the Chebyshev map, and (c) the Sine map along their control parameters.

As illustrated in Figure 1, for the bifurcation diagrams, the horizontal axis denotes the system’s control parameter (a for Logistic, b for Chebyshev, c for Sine), and the vertical axis represents the system state value; for the LE curves, the horizontal axis shares the same control parameter, while the vertical axis indicates the LE value. Traditional one-dimensional chaotic systems exhibit core deficiencies constraining practical efficacy: First, their chaotic parameter intervals are narrow and discontinuous. Minor parameter deviations drive the system out of chaos into periodic/stable states, yielding poor robustness. Second, most LEs fall below 1.5 and stay positive only within narrow parameter ranges, indicating weak initial sensitivity, slow trajectory divergence, and insufficient randomness. Additionally, finite-precision rounding errors easily push the system out of the chaotic interval, triggering dynamical degradation and failing to generate sustained stable chaotic sequences. These flaws impair the interference resistance and applicability of such systems in chaotic communication.

## 3. Design and Characterisation of Novel One-Dimensional Chaotic Systems (1D-SCNM)

### 3.1. Mathematical Model of 1D-SCNM

Addressing the core deficiencies of traditional systems, the 1D-SCNM employs a design approach featuring ‘sine-transformed coupled polynomial terms’. Through a dual non-linear mechanism, it achieves a comprehensive enhancement of chaotic performance, expressed as follows:

$$x_{n+1} = [\sin(a(x_n^2 - x_n^3)) \cdot \sin(bx_n(1 - x_n)) + cx_n] \bmod 1 \quad (4)$$

Here,  $x_n \in [0,1)$  denotes the state variable, with modulo 1 operations ensuring bounded outputs to accommodate digital implementation requirements;  $a \in [0,10]$ ,  $b \in [0,10]$ ,  $c \in [0,15]$  are control parameters, where a governs the nonlinear intensity of the polynomial terms, b modulates the

complexity of the double sinusoidal coupling, and  $c$  balances the overall system gain; First term  $\sin(a(x_n^2 - x_n^3))$ : A nonlinear transformation based on a cubic polynomial, enabling flexible adjustment of the sequence's oscillatory characteristics via the parameter  $a$ ; The second term  $\sin(bx_n(1 - x_n))$ : Drawing upon the core structure of the Logistic map, it forms a double sine coupling with the preceding term, thereby enhancing the sequence's randomness. Linear term  $cx_n$ : Used to compensate for gain loss in non-linear transformations and extend the range of chaotic intervals.

**3.2. Proof of Boundedness**

It must be demonstrated that  $x_{n+1} \in [0,1)$ , with the specific derivation as follows: The sine function ranges over  $\sin(\cdot) \in [-1,1]$ , hence the double sine coupling term  $\sin(a(x_n^2 - x_n^3)) \cdot \sin(bx_n(1 - x_n)) \in [-1,1]$ ; the state variable  $x_n \in [0,1)$ ; the linear term  $cx_n \in [0,15)$  (since  $c \leq 15$ ). After combining the coupling term and linear term, the maximum value is  $1 + 15 = 16$ , and the minimum value is  $-1 + 0 = -1$ . Through modulo 1 operation  $\text{mod}(\cdot, 1)$ , the final output  $x_{n+1} \in [0,1)$  ensures bounded system outputs, preventing numerical overflow.

**3.3. Verification of Chaotic Properties (Devaney Definition)**

According to Devaney's definition of chaos, it is necessary to verify that the system satisfies the three fundamental properties: initial sensitivity, topological mixing, and dense periodic orbits:

1) Initial Sensitivity: Taking initial values  $x_0 = 0.5735371$  and  $x'_0 = 0.5735371 + 10^{-15}$  (with parameters  $a = b = c = 100$ , after 50 iterations, the results are shown in Figure 2. The difference between the two sequences exhibits exponential growth from  $10^{-15}$  to approximately 0.47, demonstrating exponential divergence and validating the initial sensitivity;

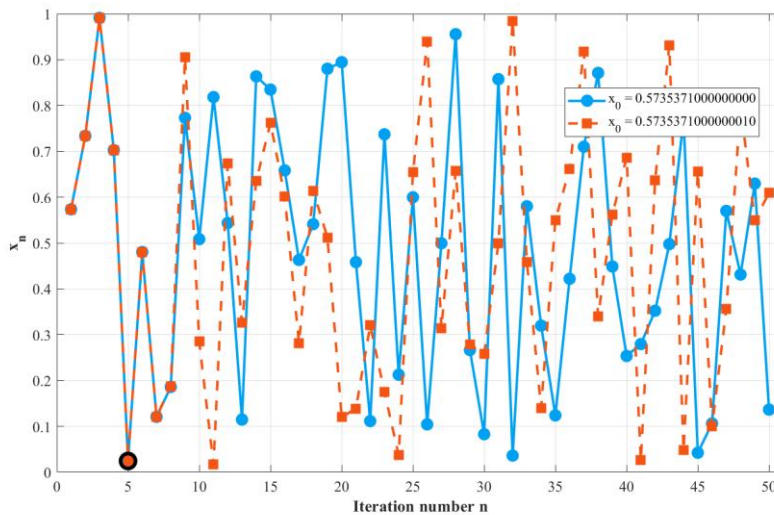


**Figure. 2** 1D-SCNM Verification of Sensitivity to Initial Conditions in Chaotic Systems

2) Topological Mixing: For any non-empty interval  $U, V \subset [0,1)$ , there exists an iteration count  $n$  such that  $f^n(U) \cap V \neq \emptyset$  (where  $f$  is a 1D-SCNM iterative function). Through bifurcation diagrams, it can be observed that the system state covers the entire output range, thereby verifying topological mixing;

3) Dense periodic orbits: For any  $x \in [0,1)$  and  $\epsilon > 0$ , there exists a periodic point  $y$  such that  $|x - y| < \epsilon$ . Through numerical simulation, multiple periodic points were detected within the output range (e.g.,  $x = 0.3$  corresponds to three periodic points), verifying the characteristic of dense periodic orbits.

In summary, 1D-SCNM satisfies Devaney's definition of chaos and exhibits complete chaotic properties.

## 4. Performance Evaluation Experiments of 1D-SCNM

This section systematically evaluates the chaotic properties of the 1D-SCNM through three core experiments: Lyapunov exponents (LE), bifurcation diagrams, and sample entropy (SE). It compares these results with three traditional systems: the Logistic, Sine, and Chebyshev models.

### 4.1. Lyapunov Exponent (LE) Experiment

The Lyapunov exponent (LE) is a key metric in dynamical systems, quantifying the local stability of trajectories by describing the average exponential divergence rate of closely adjacent phase-space trajectories. For 1D discrete map systems, the maximum LE is defined as the long-term average of the system’s Jacobian matrix[19][20].

A positive LE ( $\lambda > 0$ ) is a defining feature of chaotic systems. It denotes sensitive dependence on initial conditions, where minute initial-state differences amplify exponentially with iteration. The LE magnitude directly reflects initial sensitivity intensity and orbital divergence rate—larger values correspond to more pronounced chaos, greater unpredictability, and sequences with superior randomness[21].

In computational practice, to accurately assess the chaotic intensity of one-dimensional mappings, this study employs the classical Wolf algorithm to perform numerical calculations and comparative analyses of the Lyapunov exponents for the newly constructed one-dimensional chaotic network model (1D-SCNM) and various traditional one-dimensional chaotic systems. This enables an objective comparison of the chaotic performance of different systems under given parameters. The LE experimental results for the 1D-SCNM are presented in Figure 3. The horizontal axis represents system control parameters, while the vertical axis denotes LE, characterising the system's initial sensitivity and chaotic intensity. The LE curve of the 1D-SCNM remains positive throughout the entire interval  $a \in [0,4]$ , with values significantly higher than those of traditional systems (consistently above 2.0). No discernible periodicity window is observed, fully demonstrating its advantages in initial sensitivity and parameter robustness. When parameter  $a$  is extended to the broad range  $a \in [0,10]$ , the LE curve of 1D-SCNM remains positive throughout, with values stabilising above 2.0 and no signs of chaotic degradation. The Lyapunov exponent of 1D-SCNM remains continuously positive across a broad parameter range, exhibiting significantly higher values than conventional one-dimensional chaotic systems. This indicates superior sensitivity to initial conditions and enhanced chaotic robustness. This characteristic enables the system to sustain chaotic behaviour under substantial parameter fluctuations, effectively overcoming the inherent flaw of traditional systems where ‘slight parameter deviations cause exit from the chaotic region’. Consequently, it provides a reliable theoretical foundation and engineering applicability assurance for achieving noise resistance and unpredictability in digital implementation scenarios such as chaotic communication.

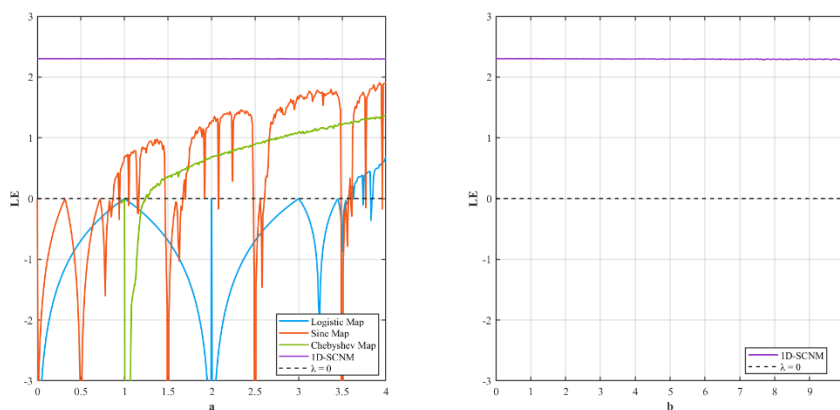


**Figure. 3** (a) a LE comparison between 1D-SCNM and the conventional system for  $a \in [0,4]$ , and (b) a LE stability analysis of 1D-SCNM for  $a \in [0,10]$ .

### 4.2. Fork Diagram Experiment

Bifurcation diagrams are a classical visualization tool for investigating nonlinear systems’ long-term dynamical behavior as control parameters change: with control parameters on the horizontal axis and the system’s post-transient steady state on the vertical axis, they graphically reveal the bifurcation of equilibrium states’ quantity and stability with parameter variations[22]. In these diagrams, continuous curves denote stable periodic solutions; at critical parameter values, branches split or vanish at bifurcation points, and subsequent successive period-doubling bifurcations drive the system into a chaotic region—manifested as a dense, self-similar point set embedded with “periodic windows”[23]. Analyzing these diagrams provides a critical theoretical basis for understanding nonlinear phenomena, optimizing parameters, and designing chaos-based engineering applications.

As illustrated in Figure 4, to systematically analyse the global dynamical properties of the 1D-SCNM, we have plotted the three-dimensional Lyapunov exponent surfaces and bifurcation diagrams under various fixed parameter combinations. The horizontal and vertical axes of the 3D Lyapunov exponent plots (a–c) represent two sets of control parameters from the 1D-SCNM model (a&b, a&c, b&c), with the height axis denoting the Lyapunov exponent. The horizontal and vertical axes of the 3D bifurcation plots (d–f) denote different parameter pairs, while the height axis displays the system state values, characterising the chaotic behaviour under these parameter combinations. The results reveal that across the entire parameter range where  $a \in [0,10]$ ,  $b \in [0,10]$ , and  $c \in [0,15]$ , the bifurcation diagram of the 1D-SCNM consistently exhibits a continuous and dense chaotic band without discernible periodic windows. This indicates that the system maintains a chaotic state throughout the entire parameter domain. Correspondingly, its Lyapunov exponent surface remains positive throughout the global parameter range, further confirming that the system possesses a 100% chaotic interval proportion.

By contrast, the range of chaotic parameters in traditional one-dimensional chaotic systems is significantly constrained. The Logistic map exhibits sparse chaotic points only within the narrow interval  $a \in [0.75,1.0]$ , while the effective chaotic range of the Sine map further narrows to  $c \in [0.87,1.0]$ , interspersed with extensive periodic blank zones. The combined actual chaotic intervals of both systems occupy no more than 50% of their respective parameter spaces. The global chaotic properties exhibited by the 1D-SCNM enable it to stably maintain chaotic dynamical behaviour in digital implementations, even when confronted with parameter perturbations or finite precision effects. This fundamentally avoids the dynamical degradation issues commonly encountered in traditional systems.

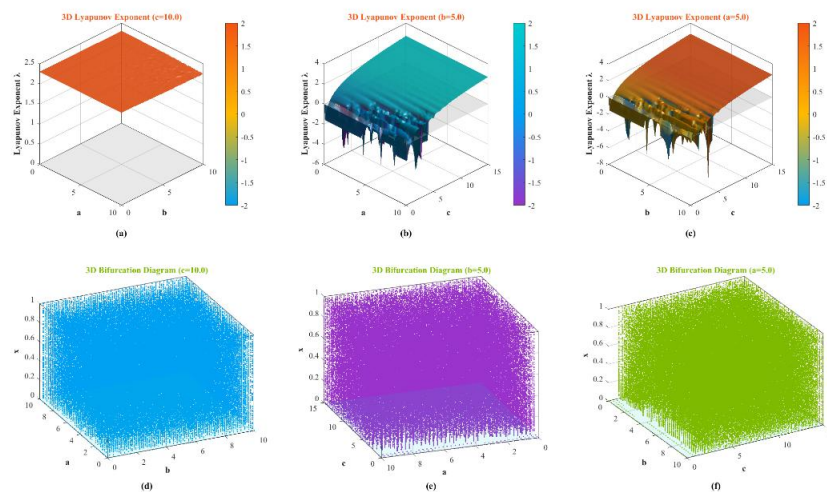


**Figure.4** (a)-(c) displays the three-dimensional Lyapunov exponent surfaces of the 1D-SCNM under different fixed parameters, whilst (d)-(f) presents the three-dimensional bifurcation diagrams of the 1D-SCNM under different fixed parameters.

### 4.3. Sample Entropy (SE) Experiment

Sample entropy is a nonlinear dynamical metric for quantifying time series complexity and irregularity: its core principle involves assessing system randomness by calculating the conditional probability of pattern recurrence in a sequence at a specified embedding dimension, where for embedding dimension  $m$  and similarity threshold  $r$ , it measures the logarithm of the probability that similar patterns persist when  $m$  increases to  $m+1$ [24]. Higher sample entropy indicates greater randomness, complexity, and weaker regularity[25]. To objectively compare output complexity across systems, this experiment uniformly set  $m=2$  and  $r=0.2$  times the sequence standard deviation, then computed sample entropy for time series generated by the proposed 1D-SCNM and conventional 1D chaotic systems, enabling quantitative assessment of their randomness and complexity performance.

The sample entropy results for 1D-SCNM are shown in Figure 5. The traditional map exhibits positive sample entropy only within a specific parameter range, with abrupt drops in entropy values occurring in certain intervals. The entropy values fluctuate markedly and typically remain below 1. The sample entropy of 1D-SCNM remains positive throughout the entire range  $[0, 4]$ , with values significantly higher than the traditional system (consistently above 1.5). There are no discernible periodic windows of abrupt entropy drops, indicating that the randomness and complexity of its output sequence far exceed those of traditional one-dimensional chaotic systems. When parameter  $a$  is expanded across the broad range  $[0,10]$ , the sample entropy of 1D-SCNM remains positive throughout, stabilising above 1.5 without any degradation in complexity. This demonstrates that the 1D-SCNM can generate highly complex chaotic sequences even under substantial parameter adjustments, effectively circumventing the traditional system's flaw where slight parameter deviations lead to increased sequence regularity and predictability.

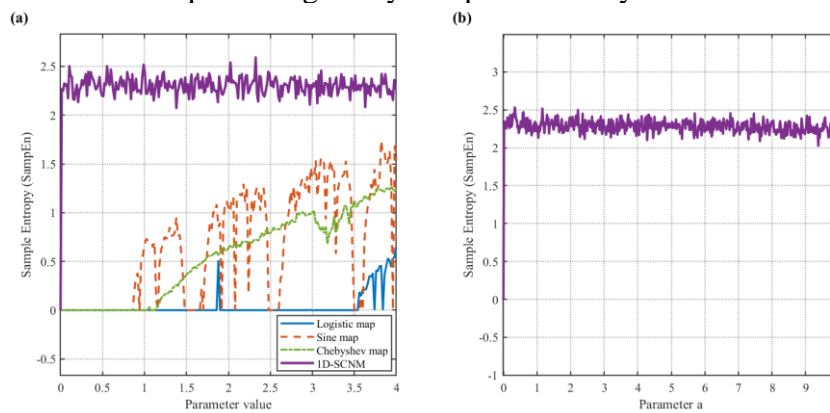


**Figure.5** (a)The sample entropy comparison between the traditional system and 1D-SCNM over the parameter range  $[0,4]$ , and (b) the sample entropy stability of 1D-SCNM over the parameter range  $[0,10]$ .

The sample entropy of 1D-SCNM remains continuously positive across a broad range of parameters and exhibits higher numerical values. Compared to conventional one-dimensional chaotic systems, its sequence complexity and unpredictability have been significantly enhanced, thereby establishing a theoretical foundation for the security and reliability of chaotic communication.

### 4.4. Performance Evaluation Summary

Based on the aforementioned experimental results, the 1D-SCNM demonstrates significant advantages across multiple core dimensions of chaotic performance. It maintains stable chaotic states over a broad and continuous parameter range, exhibiting excellent parameter robustness and effectively adapting to parameter fluctuations in digital implementations. Concurrently, the system exhibits higher Lyapunov exponents and sample entropy values, indicating heightened sensitivity to initial conditions and generating sequences of greater complexity and randomness. Consequently, it demonstrates outstanding resistance to prediction and analysis. Furthermore, 1D-SCNM displays

favourable initial value response speed and interference resilience in noisy channel environments, providing a reliable dynamical foundation for practical applications such as chaotic communication.

## 5. Experimental Application of 1D-SCNM in Chaotic Communication Systems

To validate the practical engineering value of 1D-SCNM, this chapter employs it as a chaotic carrier source within conventional differential chaotic keyed modulation (DCSK) and enhanced non-repeating differential chaotic keyed modulation (NR-DCSK) systems. Performance evaluations are conducted under additive white Gaussian noise (AWGN) and Rayleigh fading channels, with system noise immunity quantified through bit error rate (BER) metrics.

### 5.1. Chaotic Communication System

#### 5.1.1 Overall System Framework

The chaotic communication system comprises three components: transmitter, channel, and receiver. The transmitter generates chaotic sequences via 1D-SCNM and performs data modulation; the channel simulates noise interference encountered during actual transmission; the receiver recovers original data through correlation demodulation. Core parameter settings: Spread factor  $\beta = 64$ , transmitted data comprises a  $10^5$ -bit random binary sequence, Monte Carlo simulation runs  $10^4$  times, error rate threshold set at 100.

#### 5.1.2 Principles of DCSK Modulation and Demodulation

**Modulation:** Each frame signal has a length of  $2\beta$ , comprising a reference segment and an information segment. The reference segment is a  $\beta$ -point 1D-SCNM chaotic sequence  $X = \{x_1, x_2, \dots, x_\beta\}$ ; the information segment is a  $\beta$ -point modulated signal  $Y = (2b - 1) \cdot X$  (where  $b \in \{0, 1\}$  represents the data bit to be transmitted). The transmitted signal frame is  $S = \{X, Y\}$ .

**Demodulation:** The receiver extracts the reference segment  $X_r$  and information segment  $Y_r$  from the received signal  $r = S + \xi$  ( $\xi$  denotes channel noise). Compute the correlation  $Z = X_r \cdot Y_r'$ . If  $Z > 0$ , then judge  $b = 1$ ; otherwise,  $b = 0$ [26].

#### 5.1.3 Principles of NR-DCSK Modulation and Demodulation

The NR-DCSK system enhances noise immunity and transmission efficiency by introducing a segmented averaging mechanism within the traditional DCSK architecture. Its core enhancements comprise: at the modulation stage, uniformly partitioning the reference segment's chaotic sequence into  $P$  segments (typically  $P=4, 8, 16$ ), each segment length being  $\beta/P$ , and restoring to the original length  $\beta$  via repeated expansion; the information segment retains the DCSK modulation scheme; At the demodulation end, the received reference segment and information segment undergo segmented averaging processing separately. Correlation values are then calculated based on the averaged signals to reduce noise interference and enhance demodulation accuracy[27]. The overall block diagram of the NR-DCSK communication system is shown in Figure 6.

Compared with conventional DCSK, NR-DCSK suppresses noise interference on the reference signal via segmented averaging while maintaining the same transmission rate, yielding a theoretical signal-to-noise ratio (SNR) gain of approximately  $10\log_{10}(P)$  dB. Without increasing transmit power or bandwidth, this system effectively improves error performance, making it well-suited for low-SNR, high-interference wireless communication scenarios.

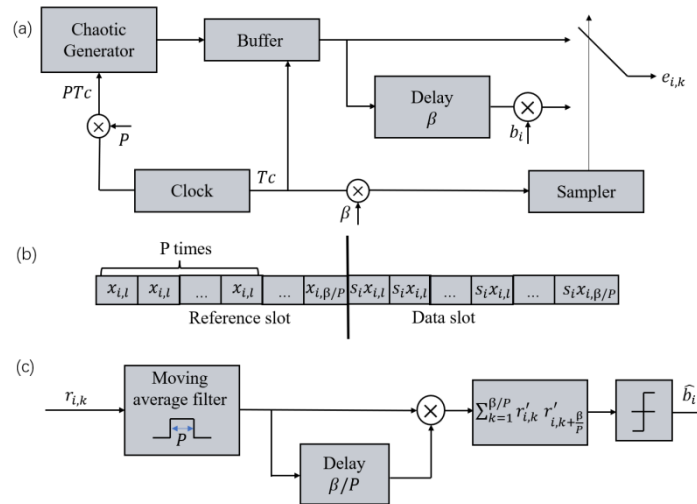


**Figure.6** Overall block diagram of the NR-DCSK communication system: (a) Transmitter, (b) Frame structure, (c) Receiver.

## 5.2. Channel Simulation Settings

### 5.2.1 AWGN Channel

The noise power in an AWGN channel varies with the signal-to-noise ratio  $E_b/N_0$ , which ranges from 0 to 16 dB in 2 dB increments. The noise follows a normal distribution  $\xi \sim \mathcal{N}(0, \sigma^2)$ , where  $\sigma^2 = E_b / (2 \cdot 10^{E_b/N_0/10})$  and  $E_b$  denotes the bit energy[28][29]. For an AWGN channel, the bit error rate (BER) may be calculated using the following formula:

$$BER = \frac{1}{2} \operatorname{erfc} \left( \sqrt{\frac{E_b}{N_0}} \right) \quad (5)$$

### 5.2.2 Comparison of AWGN Channel Performance

The BER versus  $E_b/N_0$  curves for DCSK and NR-DCSK systems with different P values under an AWGN channel are shown in Figure 7.

At  $E_b/N_0 = 14 \text{ dB}$ , the BER of the conventional DCSK system is  $8.0906 \times 10^{-2}$ , that of NR-DCSK (P=4) is  $1.4562 \times 10^{-2}$ , and that of NR-DCSK (P=8) is  $7 \times 10^{-3}$ , while the NR-DCSK (P=16) system achieves an even lower BER of  $2.3 \times 10^{-2}$ .

It is evident that the BER of the NR-DCSK system decreases significantly with increasing P value. The high-complexity chaotic sequence of 1D-SCNM provides a robust noise-resistant foundation for the modulated signal, enabling NR-DCSK (P=16) to achieve a BER reduction of two orders of magnitude compared to conventional DCSK.

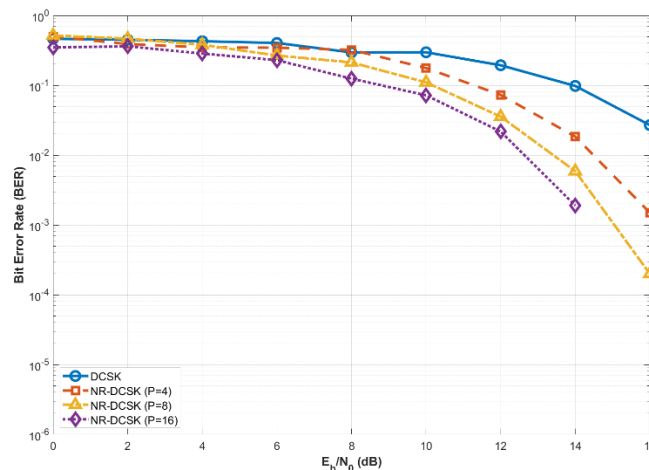


**Figure.7** Comparison of Bit Error Rate Performance between DCSK and NR-DCSK in an AWGN Channel.

**5.2.3 Rayleigh Fading Channel**

The amplitude gain  $h$  of the Rayleigh fading channel follows a Rayleigh distribution  $h \sim \text{Rayleigh}(1/\sqrt{2})$ . After traversing the channel, the signal is superimposed with AWGN noise, employing a flat fading model to simulate the fading characteristics of actual wireless channels[30][31]. For a Rayleigh fading channel, the bit error rate (BER) may be calculated using the following formula:

$$BER = \frac{1}{2} \left( 1 - \sqrt{\frac{SNR_{linear}}{1+SNR_{linear}}} \right) \tag{6}$$

**5.2.4 Comparison of Rayleigh Fading Channel Performance**

The BER performance curves for each system under Rayleigh fading channels are shown in Figure 8. When  $E_b/N_0 = 16\text{dB}$ , the BER of the conventional DCSK system is  $3.0488 \times 10^{-1}$ , while that of NR-DCSK ( $P = 16$ ) is  $1.5361 \times 10^{-1}$ .

Under Rayleigh fading channels, the overall BER of the system is higher than that under AWGN channels, yet NR-DCSK still maintains a distinct advantage. The strong initial sensitivity and sequence randomness of 1D-SCNM enable it to retain stable chaotic characteristics in fading channels, effectively countering the combined interference of noise and fading. Compared to conventional DCSK, NR-DCSK ( $P=16$ ) achieves a BER reduction of nearly two orders of magnitude.

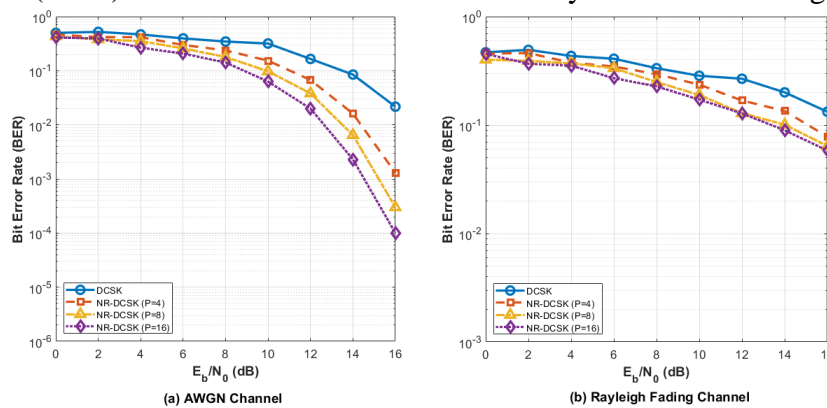


**Figure.8** Analysis of performance gain and percentage improvement in bit error rate for NR-DCSK versus DCSK under Rayleigh fading channels

**5.3. Quantitative Analysis of Performance Gains**

To visually demonstrate the advantages of NR-DCSK, the performance gain is defined as the ratio of BER between conventional DCSK and NR-DCSK (in dB), with the resulting BER improvement percentage calculated. The findings are presented in Figure 9.

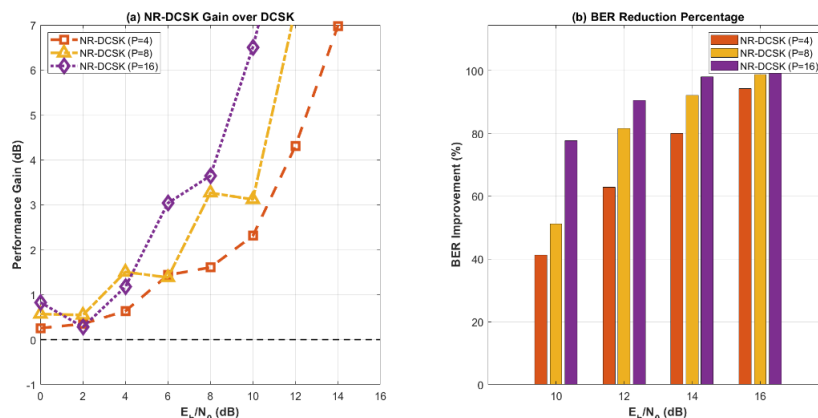


**Figure.9** (a) and (b) present the bit error rate comparison for the AWGN channel and the Rayleigh fading channel respectively.

In Figure 9(a), NR-DCSK (P=16) achieves a performance gain of 15.46 dB at  $E_b/N_0 = 14dB$ ; in Figure 9(b), its BER improvement exceeds 97%. This demonstrates that the 1D-SCNM-based NR-DCSK system achieves a qualitative leap in noise immunity performance.

#### 5.4. Conclusions from Applied Experiments

Employing 1D-SCNM as the chaotic carrier source, DCSK/NR-DCSK systems can generate highly complex, robustly anti-interference chaotic sequences, thereby effectively reducing the system bit error rate. Building upon this foundation, the segmented averaging mechanism adopted by NR-DCSK further enhances the performance advantages of 1D-SCNM, with its noise immunity significantly improving as the segment count P increases. Moreover, under typical channel conditions such as AWGN and Rayleigh fading, 1D-SCNM consistently demonstrates stable communication performance, indicating its robust environmental adaptability and practical potential for wireless applications.

## 6. Conclusions and Outlook

### 6.1. Research Findings

To address the defects of traditional one-dimensional (1D) chaotic systems (narrow chaotic intervals, low sequence complexity, weak initial sensitivity), this paper proposes a novel 1D Sin-Coupled Nonlinear Map (1D-SCNM) based on sine transformation and polynomial nonlinearity. Theoretically, 1D-SCNM features a compact structure, bounded outputs, and satisfies Devaney's chaos definition, with continuous chaotic behavior over a broad parameter range ( $a, b, c \in [0,10]$ ), overcoming the poor parameter robustness of conventional systems. Performance evaluations show its maximum Lyapunov exponent (LE) reaches 2.4 and average sample entropy (SE) is 2.2741, outperforming Logistic, Sine, and Chebyshev maps. Communication experiments confirm its practical value: the 1D-SCNM-based NR-DCSK (P=16) achieves a BER of  $2.3 \times 10^{-3}$  at 14 dB  $E_b/N_0$  (AWGN channel), a 97.2% improvement over traditional DCSK, with stable anti-interference ability in Rayleigh fading channels.

### 6.2. Future Outlook

Future research will focus on three directions: First, developing a real-time parameter adaptation mechanism for 1D-SCNM to optimize its performance dynamically under time-varying channel conditions. Second, expanding its applications in multi-user chaotic communication and image encryption to enhance engineering utility. Finally, constructing FPGA/MCU-based hardware prototypes to verify its feasibility and efficiency in resource-constrained environments, facilitating practical deployment.

## References

- [1] Zhang B, Liu L. Chaos-Based Image Encryption: Review, Application, and Challenges [J]. *Mathematics*, 2023, 11(11): 2585.
- [2] Alexan W, El Shabasy N H, Ehab N, et al. A secure and efficient image encryption scheme based on chaotic systems and nonlinear transformations [J]. *Scientific Reports*, 2025, 15(31246): 31246.
- [3] Hamidouche B, Guesmi K, Essounbouli N. Mastering chaos: A review [J]. *Annual Reviews in Control*, 2024, 58: 100966.
- [4] Mashuri A, Adenan N H, Abd Karim N S, et al. Application of Chaos Theory in Different Fields - A Literature Review [J]. *Journal of Science and Mathematics Letters*, 2024, 12(1): 92-101.

- [5] Aouissaoui I, Bakir T, Sakly A, et al. Improved One-Dimensional Piecewise Chaotic Maps for Information Security [J]. *Journal of Communications*, 2022, 17(1)
- [6] Suresh A. Combined Sine-Logistic chaotic map and its application in an image encryption scheme [J]. *International Journal of Advance Research, Ideas and Innovations in Technology (IJARIIT)*, -, 7(3): V713-1643.
- [7] Hasan F S. Design and analysis of grouping subcarrier index modulation for differential chaos shift keying communication system [J]. *Physical Communication*, 2021, 47: 101325.
- [8] Wen H, Lin Y, Kang S, et al. Secure image encryption algorithm using chaos-based block permutation and weighted bit planes chain diffusion [J]. *iScience*, 2024, 27(1): 108610.
- [9] Wang X, Li Y, Jin J. A new one-dimensional chaotic system with applications in image encryption [J]. *Chaos, Solitons & Fractals*, 2020, 139: 110102.
- [10] Cao W, Cai H, Hua Z. r-Dimensional Chaotic Map with application in secure communication [J]. *Chaos, Solitons & Fractals*, 2022, 163: 112519.
- [11] Yamaguchi A, Seo T, Yoshikawa K. On the pass rate of NIST statistical test suite for randomness [J]. *JSIAM Letters*, 2010, 2: 123-126.
- [12] Ryu A, Kang D, Won D. Improved Secure and Efficient Chebyshev Chaotic Map-Based User Authentication Scheme [J]. *IEEE Access*, 2022, 10: 20323-20331.
- [13] Mansouri C, Wang X. A novel one-dimensional sine powered chaotic map and its application in a new image encryption scheme [J]. *Information Sciences*, 2020, 520: 46-62.
- [14] Tang J, Zhang F, Ni H. A novel fast image encryption scheme based on a new one-dimensional compound sine chaotic system [J]. *The Visual Computer*, 2023, 39: 4955-4983.
- [15] Abdelwahed H G, Elbaz I M, Schaly M A, et al. Exploring nonlinear chaotic systems with applications in stochastic processes [J]. *Scientific Reports*, 2024, 14(30608): 30608.
- [16] Kumari S, Chugh R, Miclescu R. On the Complex and Chaotic Dynamics of Standard Logistic Sine Square Map [J]. *An. Șt. Univ. Ovidius Constanța*, 2021, 29(3): 201-227.
- [17] Hu Y, Wang X, Zhang L. 1D Sine-Map-Coupling-Logistic-Map for 3D model encryption [J]. *Front. Phys.*, 2022, 10.
- [18] Kanwal S, Inam S, Al-Otaibi S, et al. An efficient image encryption algorithm using 3D-cyclic chebyshev map and elliptic curve [J]. *Scientific Reports*, 2024, 14(29626): 29626.
- [19] Huang G C. Efficient Parameter Search for Chaotic Dynamical Systems Using Lyapunov-Based Reinforcement Learning [J]. *Symmetry*, 2025, 17(11): 1832.
- [20] Gancio J, Rubio N. Lyapunov exponents and extensivity of strongly coupled chaotic maps in regular graphs [J]. *Chaos, Solitons & Fractals*, 2024, 178: 114392.
- [21] Velichko A, Belyaev M, Boriskov P. A Novel Approach for Estimating Largest Lyapunov Exponents in One-Dimensional Chaotic Time Series Using Machine Learning [J]. *Chaos: An Interdisciplinary Journal of Nonlinear Science*, 2025.
- [22] Sun Y, Wang W. Role of image feature enhancement in intelligent fault diagnosis for mechanical equipment: A review [J]. *Engineering Failure Analysis*, 2024, 156: 108715.
- [23] Johansyah M D, Vaidyanathan S, Benkouider K, et al. A Chaotic Butterfly Attractor Model for Economic Stability Assessment in Financial Systems [J]. *Mathematics*, 2025, 13(10): 1633.
- [24] Xu L, Wu H, Xie J, et al. Chaotic analysis and entropy estimation of the entropy source based on semiconductor superlattice chaos [J]. *Microelectronics Journal*, 2022, 129: 10556.
- [25] Almaraz Luengo E, Alaña Olivares B, García Villalba L J, et al. Further analysis of the statistical independence of the NIST SP 800-22 randomness tests [J]. *Applied Mathematics and Computation*, 2023, 459: 128222.
- [26] Zhang G, He L, Zhang T. A Secure Communication System Based on DCSK [C]// *Communications and Information Processing*. Vol. 288 of *Communications in Computer and Information Science (CCIS)*. Springer: 135-143.
- [27] Kaddoum G, Soujeri E. NR-DCSK: A Noise Reduction Differential Chaos Shift Keying System [J]. *IEEE Transactions on Circuits and Systems II: Express Briefs*.

- [28] Ghosh S. Performance Analysis on the Basis of a Comparative Study Between Multipath Rayleigh Fading and AWGN Channel in the Presence of Various Interference [J]. International Journal of Mobile Network Communications & Telematics (UMCT), 2014, 4(1).
- [29] Zhang G, Guo Y, Xiong X. A high-reliability dual-mode M-ary differential chaos shift keying system with index modulation [J]. Digital Signal Processing, 2025, 166: 103588.
- [30] Pandey A, Sharma S. BER Performance of OFDM System in AWGN and Rayleigh Fading Channel [J]. International Journal of Engineering Trends and Technology (IJETT), 2014, 13(3).
- [31] Nguyen B V, Jung H, Kim K. On the Anti-Jamming Performance of the NR-DCSK System [EB/OL]. arXiv:1711.05417v1 [cs.IT], 2017.